

A Core-Envelope Analytic Model For The Vela Pulsar

Praveen Singh Negi

Abstract: The core-envelope models presented in Negi et al. [1]; Negi [2], corresponding to the values of compactness parameter, $u \equiv M/a = 0.30$ and 0.25 (mass to size ratio in geometrized units) have been studied under slow rotation. It is seen that these models are capable of explaining all the observational values of glitch healing parameter, $G_h = I_{\text{core}}/I_{\text{total}} < 0.55$ [3] (G_h represents the fractional moment of inertia of the core component in the starquake mechanism of glitch generation) for the Vela pulsar. The models yield the maximum values of mass, M , surface redshift, z_a and the moment of inertia for the Vela pulsar, I_{Vela} in the range $M = 3.079M_{\odot} - 2.263M_{\odot}$; $z_a = 0.581 - 0.414$; and $I_{\text{Vela},45} = 6.9 - 3.5$ (where $I_{45} = I/10^{45} \text{gcm}^2$) respectively for the values of $u = 0.30$ and 0.25 and for an assigned value of the surface density, $E_a = 2 \times 10^{14} \text{gcm}^{-3}$ [4]. The values of masses lower than the above mentioned values (so called the realistic mass range, $M = 1.4 \pm 0.2M_{\odot}$, in the literature) but significantly higher than that of the unrealistic mass range $M \leq 0.5M_{\odot}$ (obtained for the Vela pulsar in the literature on the basis of parameterized neutron star (NS) models based on equations of state (EOSs) of dense nuclear matter [3]) and other parameters may be obtained likewise for the above mentioned range of the values of G_h corresponding to the values of $u < 0.25$. The models are found to be causally consistent, gravitational bound and pulsationally stable. The upper bound on neutron star (NS) mass obtained in this study which is applicable for the Vela pulsar, in fact, corresponds to the mean value of the upper bound on NS mass obtained in the classical result by Rhoades & Ruffini [5] and that obtained on the basis of modern EOSs for neutron star matter by Kalogera & Byam [6] and is in a good agreement with the most recent theoretical estimate made by Sotani [7].

Index Terms: Static Spherical Structures, Analytic Solutions, Neutron Stars, pulsars: individual: Vela

1 INTRODUCTION

The observational data on glitch for the Crab and the Vela pulsars have been extensively studied in the literature (see, Crawford & Demiansky [3]; and references therein) which provide best tool for testing different glitch models (mechanism for glitch generation in pulsars). Since the glitch models are based on the internal structure of neutron stars, thus they can provide important information in this regard. In the starquake glitch model [8], [9] a NS is considered as a two-component structure consisting a superfluid core which consists most of the mass of the NS, surrounded by a rigid crust which contains only a few percent of the total mass. As a result of considering the thin crust in the conventional NS models, the larger value of glitch healing parameter (weighted mean value), $G_h = I_{\text{core}}/I_{\text{total}} \geq 0.7$ obtained for the Crab pulsar are easily satisfied by most of the conventional NS models in the realistic mass range ($M = 1.4 \pm 0.2M_{\odot}$)[3; and references therein]. Whereas the much lower values of glitch healing parameter (weighted mean value $G_h \leq 0.2$, obtained for the Vela pulsar could not be satisfied on the basis of starquake model unless the Vela mass falls in the unrealistic low mass range, $M \leq 0.5 M_{\odot}$ [3]. Furthermore, the estimation of core-crust boundary in the conventional NS models is somewhat arbitrary in the sense that one can freely choose somewhat lower value of the boundary (which would increase the core size) to get higher values of the glitch healing parameter, G_h , (see, e.g. [10], [11]). In order to avoid the said arbitrariness in the conventional NS models, earlier the author[12] had used a certain 'criterion' and obtained the core-envelope (instead of the term 'crust' used in the conventional NS models, the term 'envelope' is used here which includes the crust plus other interior part of the star right up to the superfluid core)

boundary of the NS models consisting a core of stiffest matter (adiabatic sound speed, $dP/dE = 1$, P and E are the pressure and energy density) and the envelope is described by the EOS of a classical polytrope. This model has been successful to explain the glitch healing parameter (weighted mean) of the Vela pulsar in the range $0 < G_h \leq 0.197$ corresponding to the realistic mass range $1.758 M_{\odot} \leq M \leq 2.2M_{\odot}$ for the Vela pulsar. Besides the two recent precisely measured larger pulsar masses about $2M_{\odot}$ ([13], [14]), the theoretical estimation indicates that the upper limit on NS mass may increase significantly from the said measured values and lie between $2.0 - 3.05 M_{\odot}$ [7]. In recent studies, Zhou et al [15] discussed the starquake model for the Vela pulsar on the basis of a solid quark star model. Lai et al [16] have proposed a strangeon star model (i.e., the solidification of the star takes place during cooling) and studied the behaviors of glitches (as result of starquake) without significant energy release, including the Crab and the Vela pulsars. By using NS observations, Steiner et al [17] obtained a crustal fraction of the moment of inertia as large as 10% for a mass $M = 1.4M_{\odot}$ to explain the glitches in the Vela pulsar even with a large amount of superfluid 'entrainment' ([18]; [19]). Delsate et al [20] have calculated the crustal moment of inertia of glitching pulsars for different unified dense matter EOSs in order to explain the large glitches observed in the case of the Vela pulsar. The present study continues to deal with the construction of such NS models which can satisfy the all observational values (not only the weighted mean values considered in the previous study) of the glitch healing parameter, $0 < G_h < 0.55$, obtained for the Vela pulsar together with the property that they may correspond to the 'realistic' mass range of NSs which ends at the value of maximum mass. The maximum value of NS mass obtained in this study may be considered identical to those obtained on the basis of modern EOSs of dense nuclear matter available the literature ([6]; [7]; and references therein). Since various observational studies and their explanation favour smooth density variation inside the NS structure ([21], [22], [23], [24]), therefore it is expected that for realistic NS models the (energy) density in the core region varies smoothly as compared to that of the outer region (envelope) where the variation of density

• Praveen Singh Negi Department of Physics, Kumaun University, Nainital – 263 002, India

becomes relatively faster. We have, therefore, considered in the present study, the core-envelope models presented in Negi et al. [1]; Negi [2] in which the density in the core is governed by the smooth variation of density (Tolman's VII solution) and the density in the envelope is described by the Tolman's V solution. The solution in the core fulfills various criteria of physically realistic structures ([25], [26]) whereas the solution considered in the envelope is found to be entirely analogous to the EOS of Wiringa et al. [27] (WFF) which is widely used in the envelope region of various NS models discussed in the literature [6] (the analogy of Tolman's V solution used in the envelope of the present study with that of the EOS WFF is explained in Sec 3). Thus, like various NS models based on EOS discussed in the literature, the models presented here, on the basis of exact analytical solutions of Einstein's field equations, are causally consistent, gravitationally bound and pulsationally stable for the allowed values of the compactness parameter $u \leq 0.30$ (Negi [2]). The distinctive feature of the models considered in the present study lies in the fact that unlike various NS models available in the literature in which the choice of the core-envelope boundary bears some arbitrariness [9], [10], the boundary of the core-envelope models presented in [1] and [2] has been obtained by an appropriate matching of all the four variables viz. pressure (P), energy density (E) and both of the metric parameters (ν and λ) at the core envelope boundary. The model yields larger values of radius for a given mass as compared to that of the previous study of the author (Negi [12]) and may provide larger values of moment of inertia for the configuration. The study carried out by Negi et al [1] deals with the construction of a core-envelope model of static and spherical mass distribution characterized by exact solutions of Einstein's field equations. The core of the model is described by Tolman's VII solution matched smoothly at the core-boundary. The region of the envelope is described by Tolman's V solution which is finally matched to the vacuum Schwarzschild solution. The complete solutions with appropriate references for both the regions (the core and the envelope) are available in Negi et al [1]. However, Negi [2] has investigated these models by removing an error in the models of Negi et al. [1] by rewriting equations (19) - (22) [as Eqs. (1) - (5) and expression for w_b as eq. (6)] in Sec. 2 of the paper (Negi [2]) with the single replacement in the symbol ' t ' \equiv ' Q ' which was assigned as a compressibility parameter in Tolman's VII solution ($\chi = r^2/K^2 = r^2/a^2 t$) discussed in Negi et al [1] and recomputed the parameters. The modified results with some other important properties of the models (adiabatic sound speed $(dP/dE)_0$ at the centre, gravitational binding energy and the pulsational stability under small radial perturbations) which were not discussed in the paper of Negi et al [1] are also included in Negi [2]. Sect. 2 of the present study deals with the relevant equations governing slow rotation of the core-envelope models presented in Negi et al [1]; Negi [2]. Results of the calculations and an application of the models to the Vela pulsar are presented in Sect.3. Sect 4 summarizes the main results of the present study.

2 EQUATIONS GOVERNING SLOW ROTATION OF SPHERICAL CONFIGURATION

The metric corresponding to a static and spherically symmetric mass distribution is given by

$$ds^2 = e^\nu dt^2 - e^\lambda dr^2 - r^2(d\theta^2 + \sin^2\theta d\phi^2) \quad (1)$$

where $G = c = 1$ (we are using geometrized units) and ν and λ are functions of ' r ' alone. The relevant equations governing the core ($0 \leq r \leq b$) and the envelope ($b \leq r \leq a$) are described respectively by Tolman's VII and V solutions of the metric (Eq.1) and are available in Negi et al [1]; Negi [2]. However, some relations relevant to the present study are redefined in the following:

$u \equiv M/a$ is the compactness parameter defined earlier and

$$M = \int_0^a 4\pi E r^2 dr$$

is the total mass; $y = r/a$ is called the radial coordinate measured in units of configuration size. The parameter n which appears in Tolman's V solution is related with compactness ratio, u , as $u = n/(2n + 1)$.

$Q (\equiv K^2/a^2)$ is defined as the compressibility factor; K is a constant appearing in the Tolman's VII solution. The matching of various parameters at the core-envelope boundary yields the ratio (b/a) , thus (b/a) represents the boundary, y_b , of the core-envelope models and ' b ' represents the core radius. For slowly rotating structures a perturbation solution for the metric (Eq.1) yields (Borner [28], Chandrasekhar & Miller [29], Irvine [30])

$$(d/dr)[F (dx/dr)] = G\chi \quad (2)$$

Where

$$F = e^{-(\nu+\lambda)/2} r^4 \quad (3)$$

(3)

$$G = 16\pi(P + E)e^{(\lambda-\nu)/2} r^4 \quad (4)$$

$$\chi = \omega - \Omega \quad (5)$$

ω being the angular velocity of structure and Ω the drag of the local inertial tetrad (Hartle & Sharp [31], Hartle [32]); known as Lense-Thirring effect.

Substituting $F (dx/dr) = \phi$ in Eq. (2) we get

$$d\chi/dr = \phi/F \quad (6)$$

and

$$d\phi/dr = G\chi \quad (7)$$

Substituting $r = ay, dr = a dy$ in Eqs. (6) and (7) we get

$$d\chi/dy = (a\phi/F) = (a\phi/a^4 f) \text{ and } (d\phi/dy) = G\chi a = a^2 g\chi a \text{ with } f = e^{-(\nu+\lambda)/2} y^4 \text{ and } g = 2(8\pi P a^2 + 8\pi E a^2) e^\lambda f \text{ or}$$

$$[d/dy](\phi/a^3) = g\chi \quad (8)$$

and

$$d\chi/dy = (\phi/a^3)/f \quad (9)$$

Substituting $\phi/a^3 = \psi$ in Eqs. (8) and (9) we have

$$d\psi/dy = g\chi \quad (10)$$

$$d\chi/dy = \psi/f \quad (11)$$

Eqs.(10) and (11) provide a set of two first order coupled

differential equations which may be solved numerically by using the standard Runge - Kutta method with boundary conditions

$$\chi_{y=0} = 1; (d\chi/dy)_{y=0} = 0 \tag{12}$$

Integrating from the centre (y = 0) to the surface (y = 1, i.e. r = a and P = 0) of the configuration, we find that at the surface

$$\omega = \chi_a + (\varphi_a/3a^3) = \chi_a + (\psi_a/3) \tag{13}$$

Drag is given by the equation

$$\Omega = \omega - \chi; \text{ or } (\Omega/\omega) = 1 - (\chi/\omega) \tag{14}$$

We define central drag as

$$(\Omega/\omega)_0 = 1 - (1/\omega); \chi_0 = 1 \tag{15}$$

Thus the surface drag is given by

$$(\Omega/\omega)_a = 1 - (\chi_a/\omega) \tag{16}$$

The moment of Inertia, I, of the configuration is given by

$$I = (\varphi_a/6\omega) = (\psi_a a^3/6\omega) \tag{17}$$

4 DISCUSSION OF RESULTS AND APPLICATION OF THE MODELS TO THE VELA PULSARS

The calculations are performed for the values of u = 0.25 and 0.30 (corresponding to the n values (1/2) and (3/4)) for assorted values of Q in the range 0.001 ≤ Q ≤ 1.3 and for an assigned value of the surface density, E_a = 2 × 10¹⁴gcm⁻³ (Brecher & Caporaso [4]). The total size of the configuration depends only on u value and turns out to be 13.369 km and 15.159 km for u = 0.25 and u = 0.30 respectively. The core size depends also on the value of Q together with u. The masses of the models depend only on u and have the values 2.263M_⊙ and 3.079M_⊙ respectively for u = 0.25 and u = 0.30. The values of (b/a), core mass, M_b/M_⊙, core size, b, boundary density, E_b, ratio of boundary density to surface density, E_b/E_a and the glitch healing parameter, G_h = I_b/I_a for the values of u = 0.25 and 0.30 are shown in Table 1 and Table 2 respectively. It may be re-iterated that the maximum permissible value of Q is obtained as 1.3 for which (b/a) ≈ 1, i.e. the whole configuration pertains to just the core solution. For Q = 0.001, we obtain (b/a) ≈ 0.029, that is the core size is much smaller and the whole configuration is dominated by the envelope solution only. Figure 1 shows the plot of moment of inertia I in units of a³ ('a' being the radius of the configuration) vs. Q for assigned values of u = 0.25 and 0.30. Figures 2 - 7 sketch the variation of relative drag (Ω/ω) vs. y, that is the change in drag from centre (y = 0) to the surface (y = 1) of the configurations for u values 0.25 and 0.30 considered in the present study and for different Q values from 0.001 to 1.3. It is seen that the central drag (Ω/ω)₀ decreases with increasing Q for both the values of u = 0.25 and 0.30. The surface drag (Ω/ω)₁ remains almost same for all the values of Q corresponding to the configurations with u values 0.25 and 0.30. It is seen from Table 1 and 2 that for Q values from 0.9 to 0.1, the core radius varies from about 83 to 29 % of the total radius of the configuration and the density at the core-envelope boundary reaches from 2.5 × 10¹⁴gcm⁻³ to 1.6 × 10¹⁵gcm⁻³. As a consequence, the fractional moment of inertia of the core component (G_h, the glitch healing parameter in the starquake glitch model) decreases from about 52 to 1.7 %

which is in excellent agreement with all the 11 measurements of G_h for the Vela pulsar (see Table 1 of Crawford & Demiansky [3]). The range of the density at the core-envelope boundary mentioned above is also found fully consistent with the range obtained by Kalogera & Baym [6] who have used the modern EOSs (two variations of WFF [18] EOS) between the said density range in the envelope region with a core given by extreme causal EOS, in context with the study of maximum mass of a NS consistent with causality and dynamical stability. The present models are also found to be consistent with causality and dynamical stability.

Table 1 The core-envelope boundary, (b/a), total radius, a, core radius, b, and the central energy-density E₀. The ratios E₀/E_b and E_b/E_a, core mass, M_b/M_⊙, and the glitch healing parameter, G_h = I_b/I_a, for the permitted value of n = 1/2 (u = 0.25) and various allowed values of Q. The value of surface density, E_a, is assumed to be the average nuclear density, like Brecher & Caporaso ([4]). For these values of u and E_a the total mass of the configuration correspond to a value of 2.263M_⊙.

u = 0.25									
Q	(b/a)	a(km)	b(km)	8πE ₀ /b ²	E ₀ /E _b	8πE ₀ /a ²	E _b /E _a	M _b /M _⊙	G _h = I _b /I _a
0.001	0.029	13.369	0.388	2.696	6.284	3205.708	765.973	0.058	0.207E-4
0.1	0.288	13.369	3.850	2.589	5.857	31.214	8.002	0.565	0.019
0.3	0.495	13.369	6.618	2.590	5.453	10.570	2.910	0.986	0.101
0.6	0.693	13.369	9.265	2.654	5.008	5.526	1.657	1.442	0.295
0.9	0.839	13.369	11.366	2.693	4.588	3.826	1.252	1.772	0.534
1.3	0.993	13.369	13.275	2.744	4.139	2.783	1.010	2.240	0.974

Table 2 The core-envelope boundary, (b/a), total radius, a, core radius, b, and the central energy-density E₀. The ratios E₀/E_b and E_b/E_a, core mass M_b/M_⊙ and the glitch healing parameter, G_h = I_b/I_a, for the permitted value of n = 3/4 (u = 0.30) and various allowed values of Q. The value of surface density, E_a, is assumed to be the average nuclear density, like Brecher & Caporaso ([4]). For these values of u and E_a the total mass of the configuration correspond to a value of 3.079M_⊙.

u = 0.30									
Q	(b/a)	a(km)	b(km)	8πE ₀ /b ²	E ₀ /E _b	8πE ₀ /a ²	E _b /E _a	M _b /M _⊙	G _h = I _b /I _a
0.001	0.029	15.159	0.440	3.044	6.289	3619.501	671.562	0.075	0.188E-4
0.1	0.287	15.159	4.350	2.878	5.676	34.940	7.183	0.714	0.017
0.3	0.487	15.159	7.470	2.964	5.267	12.170	2.698	1.282	0.093

00	93	159	2	0	9					
0.6	0.6	15.	10.	3.02		4.689	6.418	1.597	1.879	0.272
00	87	159	413	9						
0.9	0.8	15.	12.	3.11		4.263	4.523	1.238	2.392	0.518
00	30	159	580	6						
1.3	0.9	15.	14.	3.19		3.806	3.336	1.023	2.985	0.924
00	79	159	839	7						

4 SUMMARY OF THE RESULTS

The core-envelope models corresponding to compactness parameter, $u = 0.30$ and 0.25 , obtained by Negi et al [1]; Negi [2] are studied under slow rotation. The study shows that the models are capable of reproducing the all values of glitch healing parameter observed so far from the Vela pulsar on the basis of starquake glitch model. This result is in contrast to the earlier results of various studies which concluded that the starquake can not be a feasible mechanism for glitch generation in the Vela pulsar unless the Vela pulsar mass is unrealistic small. Since the matching of various parameter does not exist at the core- envelope boundary for the value of $u \equiv M/a > 0.30$, the models predict the mass, M , surface redshift, z_a , and the moment of inertia, I , for the Vela pulsar as large as $3.079M_{\odot}$, 0.581 , and $I_{\text{Vela},45} = 6.9$ respectively for the u value 0.30 and for an assigned value of the surface density, $E_a = 2 \times 10^{14} \text{gcm}^{-3}$ [4]. However the values of various parameters less than those obtained for the Vela pulsar in the present study may be obtained likewise for the same values of glitch healing parameter, G_h , by assigning the u values < 0.25 in the models described in Negi et al [1]; Negi [2]. The study further indicates that the mass, moment of inertia and compactness of the Vela pulsar may be higher than that of the Crab pulsar if the starquake is found to be the feasible mechanism in the Vela pulsar together with the Crab. Since the core-envelope models considered in the present study may reproduce the identical results on mass, radius and density range of NS models obtained by Kalogera & Baym [6] by using various EOSs in the different region of the models, it follows that the simple analytical expressions relating radial coordinate directly to the pressure, energy-density and both of the metric parameters as used here may provide important information regarding internal structure of NSs.

5 CONFLICT OF INTEREST STATEMENT

The Author declares that there is no conflict of interest.

6 REFERENCES

- [1] Negi, P. S., Pande, A. K., and Durgapal, M. C. *Gen. Rel. Grav.*, 22, 735 (1990)
- [2] Negi, P. S. *Astrophysics. Space Sci.* (Revisions are being submitted) (2019)
- [3] Crawford, F., and Demianski, M: *Astrophys. J.* 595, 1052 (2003)
- [4] Brecher, K., and Caporaso, G. *Nature*, 259, 377 (1976)
- [5] Rhoades, C. E. Jr., and Ruffini, R. *Phys. Rev. Lett.* 32, 324 (1974)
- [6] Kalogera, V. and Baym, G. *Astrophys. J.* 470, L61 (1996)
- [7] Sotani, H. *Phys. Rev. C*, 95, 025802 (2017)
- [8] Ruderman, M.: *Astrophys. J.* 203, 213 (1976)
- [9] Alpar, M.A., Chau, H.F., Cheng, K.S., and Pines, D.: *Astrophys. J.* 459, 706 (1996)
- [10] Datta, B., Alpar, M. A.: *Astron. Astrophysics.*

275, 210 (1993)

- [11] Shapiro, S.L., and Teukolsky, S.A.: *Black Holes, White Dwarfs, And Neutron Stars: The Physics of Compact Objects.* Wiley, New York (1983)
- [12] Negi, P.S.: *Mon. Not. R. Astron. Soc.* 366, 73 (2006)
- [13] Demorest P. B., Pennucci R., Ransom S. M., Roberts M. S. E. and Hessels J. W. T., *Nat.*, 467, 1081 (2010)
- [14] Antoniadis J., Freire P. C., Wex N. et al, *Sci.*, 340, 6131 (2013)
- [15] Zhou, E.P., Lu, J.G., Tong, H., Xu, R. X.: *Mon. Not. R. Astron. Soc.* 443, 2705 (2014)
- [16] Lai, X.Y., Yun, C.A., Lu, J.G., L, G.L., Wang, Z.J., Xu, R.X.: *Mon. Not. R. Astron. Soc.* 476, 3303 (2018)
- [17] Steiner, A.W., Gandolfi, S., Fattoyev, F.J., Newton, W.G.: *Phys. Rev C*, 91, 015804 (2015)
- [18] Andersson N., Glampedakis K., Ho W. C., Espinoza C. M.: *Phys. Rev. Lett.* 109 241103 (2012)
- [19] Chamel, N.: *Phys. Rev. Lett.* 110, 011101 (2013)
- [20] Delsate, T., Chamel, N., Grlebeck, N., Fantina, A.F., Pearson, J.M., Ducoin, C.: *Phys. Rev. D* 94, 023008 (2016)
- [21] Lindblom, L.: *Astrophys. J.* 278, 364 (1984)
- [22] Cottam, J., Paerels, F., Mendez, M.: *Nature* 420, 51 (2002)
- [23] Bejger, M., and Haensel. P.: *Astron. Astrophys.* 396, 917 (2002)
- [24] Haensel, P., Potekhin, A.Y., and Yakovlev, D.G.: *Neutron Stars 1. Equation of State and Structure.* Springer, Berlin (2006)
- [25] Durgapal, M.C., Pande, A.K., and Fuloria, R.S.: *Astrophysics. Space Sci.* 102, 49 (1984)
- [26] Lattimer, J.M., and Prakesh, M.: *Astrophys. J.* 550, 426
- [27] Wiringa, R.B., Fiks, V., and Fabrocini, A. *Phys. Rev. C*, 38, 1010 (1988)
- [28] Borner, G: *Springer Tracts in Modern Astrophysics*, Vol. 69, Springer-Verlag, Berlin (1973)
- [29] Chandrasekhar, S., and Miller, J. C.: *Mon. Not. R. Astron. Soc.* 167, 63 (1974)
- [30] Irvine, J.M.: *Neutron Stars*, Oxford University Press, Oxford (1978)
- [31] Hartle, J.B., and Sharp, D.H.: *Phys. Rev. Lett.* 15, 909 (1965)
- [32] Hartle, J.B.: *Astrophys. J.* 50, 1005 (1967)
- [33]

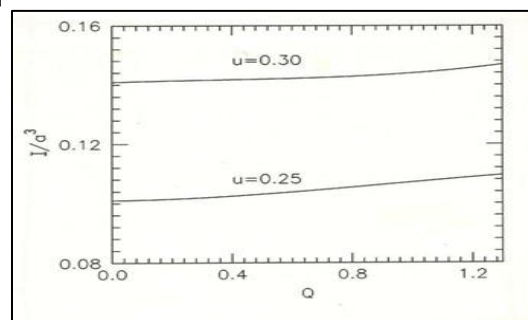


Fig. 1 Variation of l/a^3 with Q for u values 0.25 and 0.30.

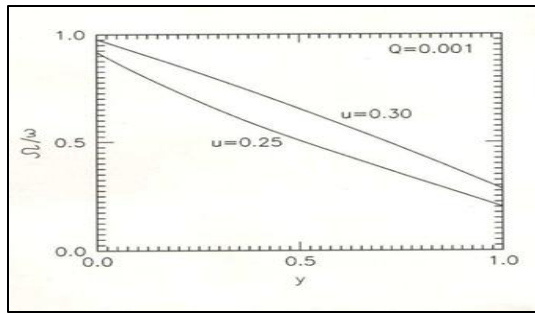


Fig. 5 Variation of relative drag (Ω/ω) vs. y , that is the change in drag from centre ($y = 0$) to the surface ($y = 1$) of the structure for the value of $Q = 0.6$ and for the assigned u values 0.25 and 0.30.

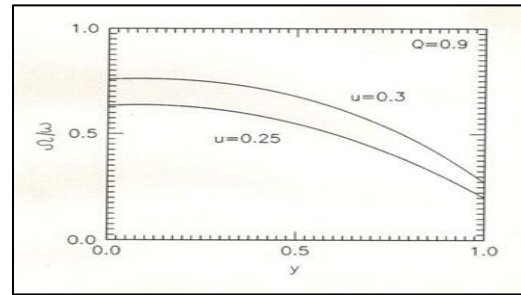


Fig. 2 Variation of relative drag (Ω/ω) vs. y , that is the change in drag from centre ($y = 0$) to the surface ($y = 1$) of the structure for the value of $Q = 0.001$ and for the assigned u values 0.25 and 0.30.

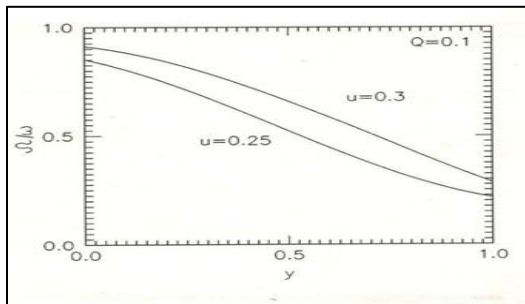


Fig. 6 Variation of relative drag (Ω/ω) vs. y , that is the change in drag from centre ($y = 0$) to the surface ($y = 1$) of the structure for the value of $Q = 0.9$ and for the assigned u values 0.25 and 0.30.

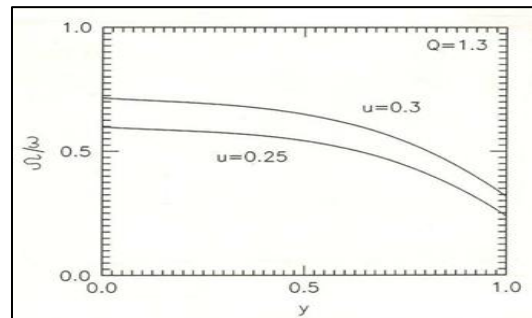


Fig. 3 Variation of relative drag (Ω/ω) vs. y , that is the change in drag from centre ($y = 0$) to the surface ($y = 1$) of the structure for the value of $Q = 0.1$ and for the assigned u values 0.25 and 0.30.

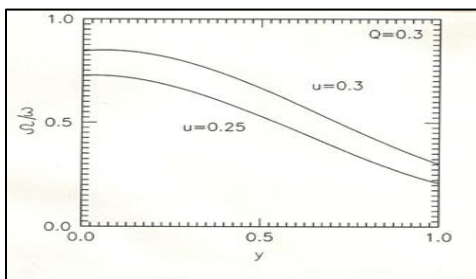


Fig. 7 Variation of relative drag (Ω/ω) vs. y , that is the change in drag from centre ($y = 0$) to the surface ($y = 1$) of the structure for the value of $Q = 1.3$ and for the assigned u values 0.25 and 0.30.

Fig. 4 Variation of relative drag (Ω/ω) vs. y , that is the change in drag from centre ($y = 0$) to the surface ($y = 1$) of the structure for the value of $Q = 0.3$ and for the assigned u values 0.25 and 0.30.

